Capt. de Corb. H. J. Goḿez Beret. The portion by Texas A and M was supported by contract Nonr 2119 (04) with the Office of Naval Research.
2. Currents were measured by steaming a number of times between the drogue and a reference buoy. Measurement of speeds involved estimates of ship's speed from normal engine turning rates and are therefore not notably accurate although directions and relative magnitudes are reliable. For discussion of drogues see G. Volkmann, J. Knouss, A. Vine, *Trans. Amer. Geophys. Union* **37**, 573 (1956).
3. W. G. Metcalf *et al., J. Geophys. Res.* **67**, 2499 (1962).
4. R. B. Montgomery, *J. Oceanogr. Soc. Japan,* 20th Anniversary Volume, 487 (1962).
5. G. Neumann, *Deep-Sea Res.* **6**, 328 (1960).
6. *Provisional Oceanographic Charts of the Tropical Atlantic Ocean* (U.S. Navy Hydrographic Office, Washington 25, D.C., 1962).

22 July 1963

Infrared Emissivity of the Sahara from Tiros Data

Abstract. *Most rocks, minerals, and sands show strong infrared reflection bands. In the atmospheric window (8 to 12μ), quartz and feldspar show an emissivity near 0.8, calcite near 1.0. These laboratory data are confirmed from observations during a Tiros flight over the Libyan desert. The Mediterranean Sea was used for calibration. Desert emissivity is between 0.7 and 0.9.*

Signals received in the 8- to 12-μ water vapor "window" radiation channel of Tiros weather satellite depend on atmospheric emission and absorption, surface temperature, and vertical surface emissivity and reflectivity in the wavelengths concerned. Vertical emissivity, ϵ, is the ratio of the vertically emitted radiant power from a source to that from a blackbody at the same temperature (and at the same wavelength). Therefore, the emissivity of a blackbody is unity. For opaque materials the verticale reflectivity is (1-ϵ). For clear air the atmospheric effect can be calculated (*1*). In the following example the atmospheric effect can be circumvented and deductions made about the emissivity of the desert surface.

Let ϵ_λ be the vertical emissivity at wavelength λ. Other subscripts refer to certain broad wavelength bands: ϵ_t = total coefficient at a certain temperature, ϵ_w for the water vapor window at 8 to 12 μ. Some data in the far infrared can be directly or indirectly evaluated from literature. Sand (*2*) of the Baltic shore has $\epsilon_t = 0.89$ at 300°K. The main constituent here seems to be quartz which has very low emission around 9 μ. This would then result in ϵ_w being close to 0.8. Similar data are found for granite, quartz, basalt, gabbro, and many other igneous rocks (*3*). Our own data show the same for feldspar.

On the other hand, water (*4*), ice, snow (*2*), vegetation, calcite, marble, and limestone (*5*), indicate $\epsilon_w > 0.95$. The emissivities for different rocks and minerals show quite complicated spectral curves. Minima of ϵ_λ for quartz and feldspar lie in the 10-μ window, but those of calcite are outside the window (*5*).

Most older meteorological literature does not consider a deviation of ϵ_t or ϵ_w from unity. The advanced state of infrared reconnaissance and the satellites demonstrates the painful lack of knowledge of ϵ data. Evaluation of infrared signals may depend more on ϵ than on temperature. At noon with the sun shining brightly a dry sand has a lower ϵ_w and a higher temperature than an adjacent wet sand. The signal from dry sand may be higher or lower than that of the wet sand depending on whether the change of ϵ or that of the temperature is more important.

The published data for ϵ_w or ϵ_t which are much lower than 0.8 seem to be erroneous: snow, 0.35 (*6*); terrain, 0.35 (*7*); gravel, plowed field and granite, 0.28 to 0.44 (*8*).

Confirmation of these statements can be found from Tiros III window observations, if proper evaluation of instrumental and atmospheric influences can be made. This has been done for orbit 44, 8 to 12 μ, 15 July 1961, 1042 to 1055 UT, a flight which has been discussed by Nordberg *et al.* (*9*). This passage covered two important areas, the Mediterranean Sea north of Libya, and the Libyan and Egyptian desert roughly between latitudes 20° and 30° N and longitudes 20° and 30° E. This desert area is known as one of the ideal deserts, free of vegetation, surface water, and people. Oases (Cufra, Siva) cover minute areas, elevations are below 400 m. On the day of this flight both areas were in, or to the east of, a weak anticyclone. No clouds were reported by ground observers or Tiros. A uniform light northerly wind had been blowing at the area for 36 hours prior to the observation. The average shelter temperature of 12 stations in the desert area (at 1300 local time) was 38°C, a figure coinciding with the average July maximum for this area (*10*).

Longer and shorter series of observations of surface versus shelter temperatures exist for about six Sahara stations (*10*, *11*). Surfaces consist of either sand or fine gravel in dry wadis. The average temperature difference in July between surface and air is 20° to 32°C at 1300 local time. The winds for this area are usually quite weak, so that it is likely the higher temperature difference might apply. On the other hand, part of the area is covered by horizontally stratified rock for which the difference might be as low as 10°C. The surface temperature, then, might be between 48° and 70°C. The air mass over the Sahara comes from the Mediterranean; hence, no water vapor could be added or subtracted to the air of this trajectory. Therefore, the attenuation of the surface radiation is almost equal over sea and land.

Water, CO_2, and O_3 vapors emit radiation to Tiros. Again, the emitted radiation was equal over land and sea for heights above 500 to 1000 m. Below this level all air layers are warmer over land and emit more. A portion $(1-\epsilon_w)$ of the atmospheric emission will be reflected by the surface and received in a somewhat attenuated form by Tiros. Effects in this paragraph would lower the computed ϵ_w even more, but they probably are small.

Therefore, we expect the Tiros record to change by an amount equivalent to a surface temperature difference of 18° to 40°C when going from sea to land. Actually, the equivalent of an 11°C change (from 288° to 299°K) was recorded by Tiros. Assuming equal atmospheric influences over sea and desert, we can from this deviation derive ϵ_w (desert) if ϵ_w (sea) is known. The ϵ_w (sea) is 0.98 for clean water (*5*) and 0.96 for water with a very thin oil layer on it (*12*). When ϵ_w (sea) = 0.98 we find ϵ_w (desert) between 0.69 and 0.91.

KONRAD J. K. BUETTNER
CLIFFORD D. KERN
Department of Atomospheric Sciences,
University of Washington, Seattle 5

References

1. S. M. Greenfield and W. W. Kellogg, *J. Meteorol.* **17**, 283 (1960).
2. G. Falkenberg, *Meteorol. Z.* **45**, 334 (1928).
3. R. J. Lyon and E. A. Burns, *Econ. Geol.* **58**, 274 (1963).
4. J. Lecomte, "Spectroscopic dans l'infrarouge," in *Handbuch der Physik* (Springer, Berlin, 1958), vol. 26, p. 2
5. K. J. K. Buettner and C. D. Kern, in preparation.
6. C. D. Miller, in *Proceedings of the Second Symposium on Remote Sensing of the Environment* (Univ. of Michigan, Ann Arbor, 1963).
7. P. Kruse, L. McGlauchlin, R. McQuistan,

Infrared Technology (Wiley, New York, 1962), p. 75
8. R. Barnes, *Science* **140**, 871 (1963).
9. W. Nordberg, W. R. Bandeen, B. J. Conrath, V. Kunde, I. Persano, *J. Atmos. Sci.* **19**, 20 (1962).
10. J. Dubief, *Le Climat du Sahara* (Algiers, 1959), vol. I.
11. K. J. K. Buettner, *Meteorol. Z.* **50**, 484 (1933).
12. E. E. Bell *et al.*, *Infrared Techniques and Measurements*, Final Eng. Rept. under contract No. 33(616)-3312, Ohio State Univ. Res. Foundation (1957).

26 August 1963

High Pressure Phases of Some Compounds of Groups II–VI

Abstract. *The high pressure phases of the mercury and cadmium sulfides, selenides, and tellurides have been determined by means of x-ray diffraction patterns obtained while the materials are under pressure.*

The effect of high pressure on the properties of many of the Group II–VI compounds has been the subject of many recent discussions (*1*, *2*). The most pronounced effects of pressure have been the drastic changes in the electrical resistances of the materials, and these changes are again attributed to crystallographic transformations (*3*). In some cases, direct evidence of the transformation has been obtained from x-ray diffraction patterns taken while the material is under pressure (*4*). However, the new structures are usually based on the appearance of a rather limited number of x-ray reflections.

Table 1. Lattice parameters of atmospheric and transformed phases crystal. Structure: B_1 cubic NaCl type; B_3, cubic zinc-blende type; B_4, hexagonal wurtzite type; B_9, hexagonal cinnabar type.

Compound	Atmospheric phase		High pressure phase		Applied pressure* (kb)
	Crystal structure	Lattice parameters a_0 – – – c_0 (A)	Crystal structure	Lattice parameters a_0 – – – c_0 (A)	
HgS	B_3	5.85	B_9	4.15–9.50	—
HgSe	B_3	6.09	B_9	4.32–9.68	15
HgTe	B_3	6.44	B_9	4.46–9.17	20
CdS	B_4	4.14–6.72	B_1	5.32	33
CdSe	B_4	4.30–7.01	B_1	5.49	32
CdTe	B_3	6.46	B_1	5.81	36

* As calculated from gas pressure applied to piston.

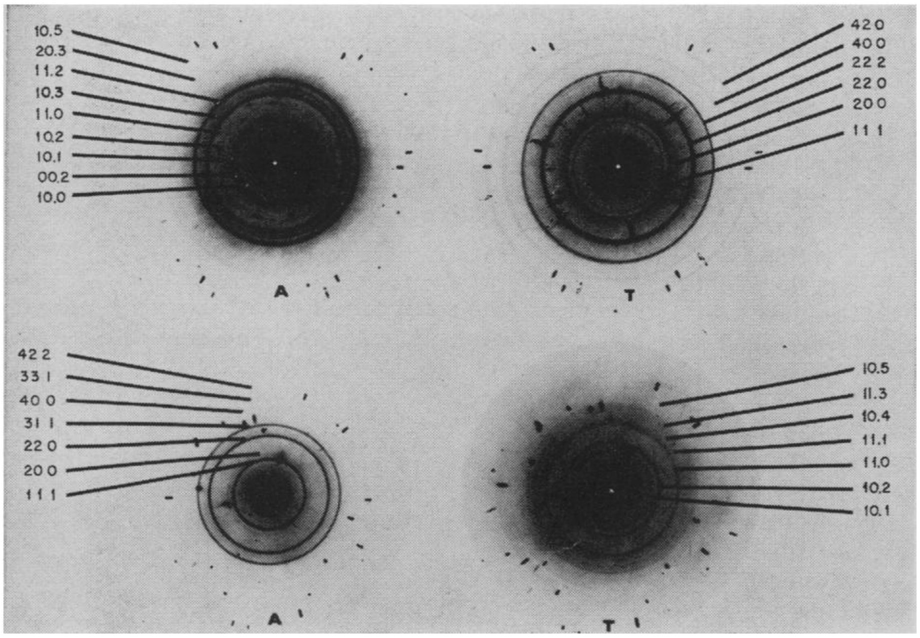

Fig. 1. X-ray diffraction patterns. Top *A*, CdSe at atmospheric pressure; Top *T*, CdSe at 32 kb; Bottom *A*, HgTe at atmospheric pressure; Bottom *T*, HgTe at 20 kb.

This report presents a series of x-ray parameters for some Group II–VI compounds that were obtained on an x-ray pressure camera similar to that described by Piermarini (*5*). However, the camera was modified by the addition of a film cassette whereby higher resolution patterns can be obtained over a larger angular range. With molybdenum radiation and the modified cassette, 2θ angles of about 40 degrees were recorded on films about 10 cm in diameter. The camera constant was calculated by using the untransformed x-ray diffraction pattern as a standard. Typical x-ray diffraction patterns with (*hkl*) indices, superimposed on the Laue pattern from the diamond anvils, are shown in Fig. 1.

The pressure was applied to the samples, held between two diamond anvils, by means of a gas-activated piston arrangement. The applied pressures were calculated from the known radii of the piston and diamond-bearing surfaces. The calculated values and comparisons with known transformation points from electrical data indicated ranges of 40 to 50 kb could be obtained with standard compressed gas cylinders. No attempt was made to measure the actual pressures in the camera except to apply sufficient pressures to cause the transformation.

The x-ray parameters and type of crystal structure obtained for a series of Group II–VI compounds are presented in Table 1.

These data are in fair agreement with parameters published for CdS and CdSe, 5.30 Å and 5.54 Å, respectively (*4*). It is difficult to ascribe any significance to the slight discrepancies because of inherent errors in attempting to measure pressure gradients over such small areas. No attempts have been made to correct the lattice parameters for compressibility effects of the transformed phase. The apparent inconsistency of the C_0 parameter of mercury telluride compared to the parameters of other mercury compounds does, however, indicate that compressibility could be responsible for the smaller C_0 parameter.

The cadmium compounds, representing both zinc-blende and wurtzite structures at atmospheric pressure, transformed into cubic NaCl-type structures. The mercury compounds, all zincblende structures at atmospheric pressure, transformed into the distorted NaCl-type or cinnabar structure. The